Application of integrated forward and reverse osmosis for coal mine wastewater desalination

CrossMark

Ramesh Thiruvenkatachari *, Mathew Francis, Michael Cunnington, Shi Su *

Commonwealth Scientific and Industrial Reserach Organisation (CSIRO), 1 Technology Court, Pullenvale, Queensland 4069, Australia

ABSTRACT

Water management is an integral part of coal mining operations. Due to the constraints on releasing saline water, coal mines require additional water storage facilities and therefore seek to minimise their inventory of saline water. Adopting efficient treatment technologies on-site would minimise the risk of wet season run-offs, freshwater contamination and allow segregation of different qualities of water to enable greater water recycling. This study aims to evaluate the application of an integrated forward osmosis (FO) and reverse osmosis (RO) system with three different actual coal mine waters, containing various concentrations of sulphates and silica that are generally associated with scaling and fouling of membrane systems. Three different FO draw solutions, di-sodium hydrogen phosphate (DHSP), sodium hexametaphosphate (SHMP) and sodium lignosulphonate (SLS) were evaluated. Two different modes of integrating the FO and RO systems were identified. The integrated system was able to concentrate the brackish mine waters, recovering more than 80% of the volume of mine water and obtaining dischargeable quality treated water. Simple physical cleaning with clean water circulation was found to be effective in restoring the FO water flux. The osmotic gradient between two mine waters was also utilised to adopt mine water as a draw solution. The effect of solution temperature on stand-alone and integrated FO and RO systems was also evaluated. The combination of FO with RO provided a better performance than individual FO or RO in treating coal mine wastewater. The FO unit served as an effective pre-treatment system prior to RO and the integrated FO–RO systems has a strong potential to successfully eliminate conventional pre-treatment processes for RO.

© 2016 Elsevier B.V. All rights reserved.

1. Introduction

Water resources in Australia face an enormous challenge in maintaining a sustainable balance between the amount of water extracted from water sources and ensuring appropriate environmentally safe flows. The problem is exacerbated due to the variability in climatic conditions [1,2]. Water is an integral part of various industrial operations, including coal mining, and is obtained from a variety of sources like ground water, surface water (rainfall and runoff) and fresh water from mains supply. Adopting efficient treatment technologies to reuse and recycle the water that is generally stored on-site after mining operations, is one of the effective water management strategies to minimise the risk of wet season run-offs and reduce the pressure on our water resources and the environment. A recent study on the water quality of mine water from different coal mines in Australia [3], has

shown significant variation in the characteristics of mine water. The pH of the water sources ranged from acidic to basic in nature. Some streams showed higher dissolved solids concentration than the other and had the characteristics of fouling and scale formation.

Reverse osmosis (RO) is a mature process and one of the most commonly used desalination technologies in Australia [4] and more than 50% of the world's desalination water is produced by the RO process [5,6]. However, RO membranes can be very sensitive to fouling by various dissolved and undissolved constituents, particulate matter, salt precipitates, microorganisms, and would require extensive and expensive pre-treatment to ensure acceptable performance [7–11]. Currently, coal mine affected water is extensively pre-treated prior to RO treatment. The pre-treatment processes include lime neutralisation to adjust the pH, coagulation and precipitation where suspended solids, excess lime, some precipitated metal elements and gypsum are removed, multimedia filters to further reduce the concentration of suspended solids, membrane filtration units to reduce colloidal material and water softeners to reduce hardness and the addition of antiscalents prior

to RO treatment. This pre-treatment process comprises 10–36% of the total operating cost [10,12].

The forward osmosis (FO) process is an emerging low energy desalination technology [13–15], where water naturally traverses the semi permeable membrane (osmotic pressure is the driving force, instead of hydraulic pressure) from a lower solute concentration feed solution to a higher solute concentration solution, known as the draw solution. Clean water is then recovered from the diluted draw solution using a post treatment step [16], although direct application of fertiliser based draw solutions have been attempted [17,18]. The bulk of the research has focused on FO membrane development [19–24] and new draw solutions [18,25–28]. Reviewing the literature over the last decade, Lutchmiah et al. [29] reported that only 7% relate to applications for treating various wastewaters. Its application as a separation process for the treatment of complex wastewaters includes drilling mud and fracturing fluids from oil and gas operations [30,31], nutrient rich streams (centrate) [32], municipal wastewater [33,34], power plant wastewater [35], coke-oven wastewater [36], textile dye effluents [37], dewatering RO concentrate [38]. However, studies on the application of forward osmosis for coal mining impacted water are scarce [39,40]. Hybrid systems whereby FO is combined with thermal processes [31,41,42] or other membrane treatment methods like ultrafiltration, nanofiltration and reverse osmosis [27,43–45], have been adopted, generally replacing either chemical pre-treatment, or used to reduce the volume of the waste stream as a post treatment step. Particularly, studies on FO–RO combined systems have focused in treating NaCl solutions, secondary/tertiary treated effluent [44,46] or seawater [47–50]. This study aims to apply an integrated forward and reverse osmosis process in treating three different types of coal mine impacted waters.

2. Materials and methods

2.1. FO and RO experimental set-up

The fabricated bench scale forward and reverse osmosis systems used in this study are shown in Fig. 1. The forward osmosis unit consists of a membrane cell with an effective membrane area of 150 cm². Inlet and outlet ports were provided on both sides of the FO membrane cell to allow the circulation of feed water on one side and draw solution on the other side of the membrane using two variable speed peristaltic pumps (Longer Pumps, YT600-1J). A co-current cross-flow mode of operation was adopted throughout the study. The change in weights of the feed and draw solutions was monitored using weighing balances (Wedderburn Scales, Vibra AJ) and were data logged (Wedderburn, DI- Connect,

version 1.5) with a time interval of 10 s. The temperature of the solutions were maintained at a set value (with variation of ±0.5 °C) using a water circulation bath (Thermoline Scientific BL-30). The pH and conductivities of the solutions were measured using a WP-81 analyser with $K = 1$ and K10 probes (TPS Australia Pty. Ltd.) and data logged every 10 s (WinTPS, version 1.35). The energy consumption of the FO unit was monitored using a power meter (CABAC Power Mate 10 A).

For the FO operation, water flux Jw (in $Lm^{-2} h^{-1}$) across the membrane was calculated from the change in volume (calculated from the weight change) of the draw/feed solution per unit time and for a given unit membrane area. An important aspect of the draw solution in the FO process, apart from its ability to produce higher water flux, is the amount of draw solute transport in the reverse direction to the water flux. Reverse solute flux (RSF), Js, which is the flux of salts through the membrane from the draw solution to feed solution, and the specific reverse solute flux (SRSF), which is the ratio of RSF to the flux of water through the membrane in the forward direction (Jw) [51,52] were determined. SRSF yields a salt transport (crossing the membrane from the draw solution to the feed solution) in grams per litre of water being produced (from feed solution to draw solution).

The RO unit consists of a membrane cell with an effective membrane area of 140 cm². A diaphragm pump (Hydracell DO3X) with a variable speed drive (VSD) was used to circulate the water through the cell. The required operating pressures were set using a pressure regulating valve and a needle valve. Pressure sensor (Keller ECO1), flowmeter (Blue-White Industries F-550) and pressure relief valve (DK-Lok D-Pro V66 Series) were installed inline. The energy use of the RO system was monitored from the VSD through the LabVIEW software computer programme.

Initially, experiments were carried out with FO as standalone process and then integrated with the RO system for the regeneration of draw solution and recovery of clean water from mine impacted water.

2.2. FO and RO membrane characteristics

Commercially available flat sheet FO membrane (Hydration Technology Innovations (HTI), Albany, USA) and polyamide FILM-TEC brackish water RO membrane (BW-30) were used in this study. The FO membrane is a cellulose triacetate membrane embedded about a polyester screen mesh with a rejection layer and a support layer. The thickness of the membrane was measured using a micrometer Mitutoyo thickness gauge (Japan) and was found to be 90 ± 3 μm for FO membrane and 150 ± 2 μm for RO membrane. The pure water permeation coefficient for FO membrane was found to be $0.976 \, L \, m^{-2} \, h^{-1} \, bar^{-1}$ and the RO membrane was $2.4 \, L \, m^{-2} \, h^{-1} \, bar^{-1}$.

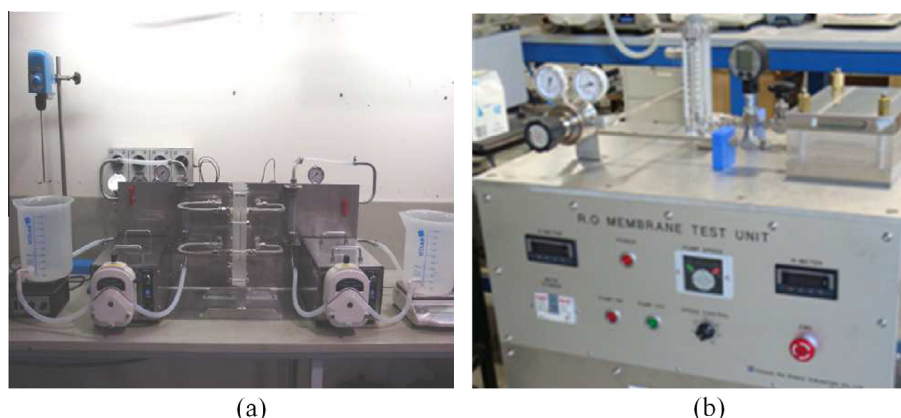(a)   (b)

Fig. 1. Photo of the lab scale flat sheet (a) FO and (b) RO test units.

Table 1
Characteristics of three different coal mine impacted waters.

Characteristics	Units	MW1	MW2	MW3
pH		7.6–7.7	7.6–8.0	6.8–7.5
Conductivity range	$\mu S\ cm^{-1}$	970–1500	9000–11,000	17,000–18,500
Carbonate/bicarbonate	$mg\ L^{-1}$	153	270	27
Calcium	$mg\ L^{-1}$	19	177	508
Magnesium	$mg\ L^{-1}$	24	253	531
Sodium	$mg\ L^{-1}$	162	2010	4800
Chloride	$mg\ L^{-1}$	218	1370	1030
Sulphate	$mg\ L^{-1}$	41	3260	12600
Potassium	$mg\ L^{-1}$	4	15	124
Strontium	$mg\ L^{-1}$	0.508	6.81	2.6
Manganese	$mg\ L^{-1}$	0.185	0.015	9.67
Silica	$mg\ L^{-1}$	–	<0.5	15
Iron	$mg\ L^{-1}$	0.9	0.28	<0.5

2.3. Feed and draw solutions

Three coal mine water sources with different water quality characteristics, from open cut and underground coal mines in Australia (two from Queensland and one from New South Wales), were used as feed waters in this study and are represented as MW1, MW2 and MW3. pH, conductivity and the composition of the mine impacted water are reported in Table 1.

The three draw solutions used in this study were sodium hexametaphosphate (SHMP) (trade name Calgon T), sodium lignosulfonate (SLS) and di-sodium hydrogen phosphate (DHSP) (Albright & Wilson, Australia). These substances are used in various industrial applications [53–56]. Sodium phosphate is an anti-caking and anti-scaling agent; sodium hexametaphosphate is one of the food additives and is used in water softening, as deflocculant and for dispersion of ores and clay. Purified technical grade powdered sodium lignosulphonate is derived from spruce wood and is used as a dispersing agent in water treatment. Sodium chloride (Sigma Aldrich, Australia) was used as a reference solution. Milli-Q (Merck Millipore Direct-Q 5UV) water was used to make up the draw solutions and reference solutions.

The osmotic pressure of some draw solutions can generally be theoretically calculated using commercial software, for example OLI Stream Analyzer™ [25,57,58]. This software uses thermodynamic data to predict the properties of the solutions over a wide range of concentrations and temperatures. However, in this study, the osmotic pressure of the three draw solutions used were obtained experimentally using the FO system. The draw solution with unknown osmotic pressure was introduced as the feed solution to one side of the FO membrane against sodium chloride with known osmotic pressure as the draw solution on the other side of the membrane. The concentration of the sodium chloride on the draw side was gradually reduced with each subsequent experiment while the concentration of the feed solution was kept constant. Eventually there is a point where no permeate would flow across the membrane and at this point the osmotic pressure of the feed solution is equal to the osmotic pressure of the sodium chloride draw solution. The osmotic pressure of sodium chloride solution was calculated using the Morse equation [59–61].

3. Results and discussion

3.1. Individual FO and RO operations

The osmotic pressure data obtained experimentally for the three draw solutions used in this study is given in Table 2. The FO fluxes and reverse draw solute diffusion characteristics identified for the three draw solutions are given in Table 3.

Among the three draw solutions studied, although the osmotic pressure of SLS was significantly higher than SHMP and DSHP, there was only a small increase in its flux compared to the other two. RSF for DSHP was the lowest, followed by SLS and SHMP. Membrane surface charge, hydrated diameter of the ionic species and association of ions are some of the effects known to have an influence on the amount of reverse solute permeation [17,51]. With the three draw solutions having similar flux values, the SRSF also followed a similar trend as RSF.

The salt rejection performance of the FO membrane for the three mine waters was evaluated by inserting the FO membrane in the RO unit and then applying different operating pressures, similar to the method of operation with a brackish water RO membrane. The salt removal efficiency of the FO membrane for three different mine waters (Table 4) was consistently high at about 87–89%, even with the variation in salt concentration in the feed mine water.

Overall, the salt rejection efficiencies of the FO membrane was similar or better than the performance of the RO membrane, which had rejection efficiencies ranging from 85% to 90% at a pressure of 20 bar.

The effect of membrane orientation was also studied with the two different mine waters. Fig. 2 demonstrates the effect of membrane orientation on water flux for MW2 and MW3 using the draw solution SHMP. As expected, difference in water flux was noticed depending on the orientation of the membrane surfaces (active layer and the support layer) to the feed and draw solutions. The variation in the solute concentrations (feed and draw solution side) at the membrane boundary layer (concentration polarisation

Table 2
Osmotic pressure at 25 °C for 0.25 M concentration draw solutions.

Draw solutions (conductivity, $mS\ cm^{-1}$)	Osmotic pressure, atm
DSHP (32.7)	15.50
SHMP (40.1)	17.39
SLS (44.7)	33.50

Table 4
Salt rejection efficiencies of the FO membrane for three types of mine impacted waters (applied pressure 20 bar).

Feed water type	Feed water conductivity, $\mu S\ cm^{-1}$	Permeate quality, $\mu S\ cm^{-1}$
MW1	1080	115
MW2	10,350	1365
MW3	18,500	1940

Table 3
FO fluxes and reverse solute diffusion characteristics of three draw solutions.

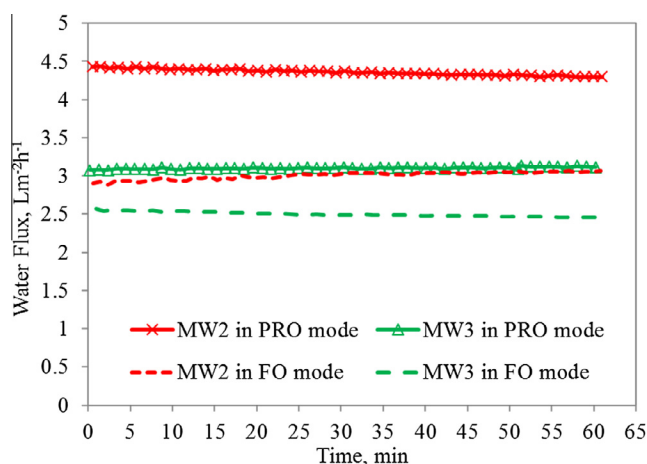| Draw solution (0.25 M concentration)	FO flux (Jw), $Lm^{-2}\ h^{-1}$	Reverse solute flux (Js), $g\ m^{-2}\ h^{-1}$	Specific reverse solute flux (Js Jw^{-1})
DSHP	6.05	30.93	5.11
SHMP	5.83	125.65	21.55
SLS	6.97	71.82	10.30

Fig. 2. Effect of membrane orientation on water flux (draw solution: SHMP with initial concentration 0.25 M, flow rate 1 L m^{-1}, cross flow co-current direction).

effects) influences the net osmotic pressure, which determines the water flux for two different membrane orientations [62,63].

During the course of this set of experiments the feed solution concentration was kept constant for both orientations in order to minimise the concentration polarisation effects. When the brackish mine water was used as the feed solution facing the membrane active layer (FO mode), a concentrative external concentration polarisation (ECP) occurs on the active layer side as the solute is concentrated at the membrane surface and a dilutive internal concentration polarisation (ICP) on the membrane support layer side as the draw solution is diluted by the permeate water within the porous support of the membrane. When the membrane active layer faces the draw solution (pressure retarded osmosis- PRO mode), the phenomenon is dilute ECP on the active layer side and a concentrative ICP on the porous support layer as the concentration of salt from the feed solution increases within the porous support layer as it cannot pass through the active layer [64]. Although concentrative ICP occurs on the feed side of the membrane, its effect is less pronounced than dilutive ICP and so the flux is higher when membrane active layer faces the draw solution than when it is towards the feed solution [17]. However, for practical applications, the preferred orientation in treating mine waters would be having the membrane active layer towards the feed mine water, even though it results in slightly lower water flux compared to other orientation. This can be further supported from Fig. 2 as the difference in water flux between the two modes of operation was lower for mine water MW3 with higher dissolved solids concentrations of sulphate and silica, compared to MW2.

The draw solutions were passed through the reverse osmosis unit to determine the quality and quantity of permeate produced. The RO permeate flux at 30 bar and the RO permeate conductivity for 0.25 M concentrations of the draw solutions tested are presented in Table 5.

Although SLS had the highest FO flux among the three draw solutions, it has a very low RO flux (at 30 bar), due to its high osmotic pressure. While draw solutions with higher osmotic

pressure are generally an advantage for the FO, careful consideration is required in selecting the osmotic gradient for an integrated FO–RO system.

3.2. Integrated FO/RO experiments

In this study, two different modes of integration of FO and RO units were evaluated in treating the coal mine impacted waters. Simple schematics of the two modes of FO–RO integration are shown in Figs. 3 and 4. The flow rates of the FO and RO units were balanced in two ways. In the first, the flow rate of the RO was matched to the flow rate of the FO draw (including the FO permeate flux). This is referred to as 'matched volume integration mode'. In this mode, the concentration of the draw solution gradually increases (as the feed is also being concentrated).

In the second integration mode, the focus was on keeping the concentration of the draw solution constant by repeated additions from the RO reject stream (the draw volume may or may not be kept constant). This is referred to as 'constant draw concentration integration mode'.

Table 6 gives the summary of performance obtained through the two modes of FO–RO integration. The results of the integration experiments presented in Table 6, using mine impacted water MW2 as feed and the three draw solutions, shows the average permeate flux rates from FO and RO units and RO rejection over four hours of operation.

The integration work demonstrated that each integration mode has an advantage over the other mode. The matched volume mode, the configuration with which most current hybrid systems operate with, completely integrates both of the two treatment methods, thus reducing the volume of water that is not utilised. Lower recoveries were seen with the matched volume mode, due to the lower operating RO pressure. A scaled up system with a higher FO membrane footprint would require a higher RO operating pressure to match the increased FO permeate rate which would lead to an increase in permeate quality. The constant draw concentration mode only utilises a fraction of the reject stream with the remainder still being sent for disposal or further treatment but does
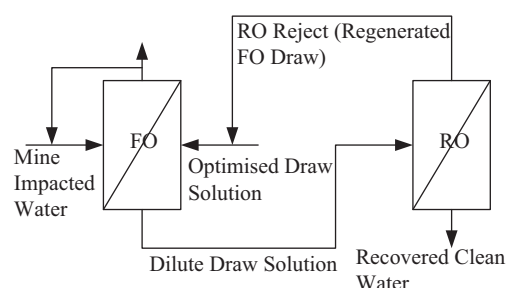

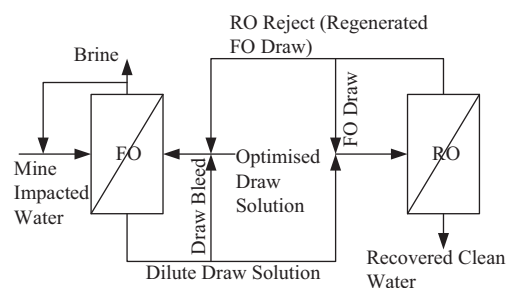**Fig. 3.** Schematic of matched volume integration mode.

Fig. 4. Schematic of constant draw concentration integration mode.

Table 5
RO performance with three different draw solutions.

Solution (0.25 M concentration)	RO permeate flux, Lm^{-2} h^{-1} at 30 bar	RO permeate conductivity, µS cm^{-1} at 25 °C
SLS	0.5	7,230
DSHP	10.8	404
SHMP	11.1	315

Table 6
Performance comparison of two modes of FO–RO integration (FO feed MW2, starting draw conductivity 30 mS cm^{-1} at 25 °C).

| Integration mode	Draw solution	FO permeate flux, Lm^{-2} h^{-1}	RO pressure, atm	RO permeate flux, Lm^{-2} h^{-1}	RO rejection, %
Matched volume	DHSP	3.3	8	2.2	85.39
	SHMP	2.4	7	1.7	75.4
	SLS	4.0	23	3.9	96.3
Constant draw concentration	DHSP	3.2	25	15.6	97.35
	SHMP	2.4	25	16.0	98.09
	SLS	4.0	25	5.9	97.37

produce a higher volume of high quality water. Another advantage of the constant draw concentration mode is that it is easily retro-fittable onto existing RO plants. These two different modes could be utilised at different times of the years as discharge conditions vary and selected based on feed water characteristics, available osmotic gradient and required treated water quality.

The SLS constant draw concentration integration experiment delivered the highest FO permeate flux rate of 4.0 Lm^{-2} h^{-1}, yet SHMP had the best RO rejection rate of 98.09%. This confirms that SLS, with the highest osmotic pressure, delivers the highest FO permeate flux rate but due to this high osmotic pressure the RO rejection rate seen for this draw solutions is lower than for other draw solutions. SLS was also found to discolour the FO feed solution, making it an unlikely choice for use as a draw solution in future.

Following the examination of the two separate modes of integration, two different mine waters were treated using the FO–RO process with one mine water acting as the FO feed and the other acting as the FO draw/RO feed. Although the osmotic gradient between the mine waters tested is not large, it opens up the possibility of applying one mine water to treat the other, particularly where two mines are in close proximity with mine waters of different concentrations. The integration mode selected for this experiment was constant draw concentration and the variation in the feed and draw concentrations were observed pre and post integration (Fig. 5) over the course of about eight hours of operation.

The rate at which the FO feed concentrated at prior to integration (with the draw constantly diluting) was 0.11 μS min^{-1}, while with the draw concentration was held constant (post integration with the RO), when the feed was found to concentrate at a rate of 0.16 μS min^{-1}. This shows an increase in the permeate concentration rate of 45% after the integration with RO system even after the feed solution has already been concentrating for four hours, which would have reduced the starting osmotic gradient. The RO performance was found to be consistent with over 98% rejection at 25 bar and an average flux of about 15 Lm^{-2} h^{-1}.

The integrated FO and RO units were also run for a more prolonged period (duration of 15 h in three block of 5 h of each operation) using the higher dissolved solids containing MW3 feed solution (which contains inorganic foulants such as sulphate and silica) and 0.25 M SHMP draw solution under FO mode. The FO and RO were integrated in constant volume but with a higher RO pressure so that a higher concentration of RO reject would be returned to the draw solution and thus keep the osmotic gradient between the FO feed and the FO draw constant, leading to a constant FO flux rate. The FO membrane was not rinsed after the first block of 5 h, but was rinsed by circulating clean water on both sides of the membrane after 10 h of operation. No other form of cleaning was employed during the course of this study. After the first 10 h of operation without any cleaning of the FO membrane, the flux dropped by 11% of the starting flux rate. However, upon simple rinsing of FO membrane with clean water, the original, starting flux rate was achieved. The reversibility of water flux decline in FO process by simple physical cleaning has previously been demonstrated in detail [30,65]. This effect can be attributed to the less cohesive and loose layer of deposit formed on the
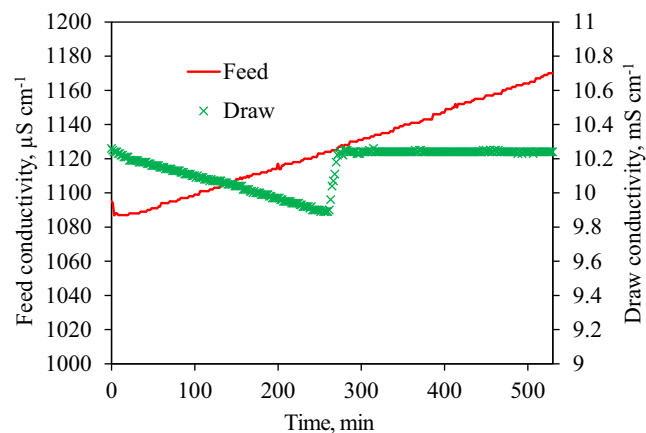
Fig. 5. Conductivity trends in FO during pre and post integration (feed solution MW1, draw solution MW2).

osmotically driven membrane that is able to be removed by physical cleaning. Fig. 6 presents the results for the operation of the RO unit in regenerating the draw solution SHMP during the 15 h of operation of the integrated system.

The RO permeate flux was steady with a slight decline as the RO feed concentration increased over the course of the experiment. Under the study conditions adopted, the RO flux rate was more than twice the FO flux rate but even over the course of the study period this had no significant effect on the integrated system (due to the disparate volumes of the FO and RO feed). However, under the field conditions the volume lost from the RO feed through the higher permeate rate could be made up with the diversion of a higher volume of waste brine or by having a larger capacity FO unit. Fig. 6 also demonstrates that during the course of 15 h of operation, the overall efficiency of salt removal was consistently over 96%.
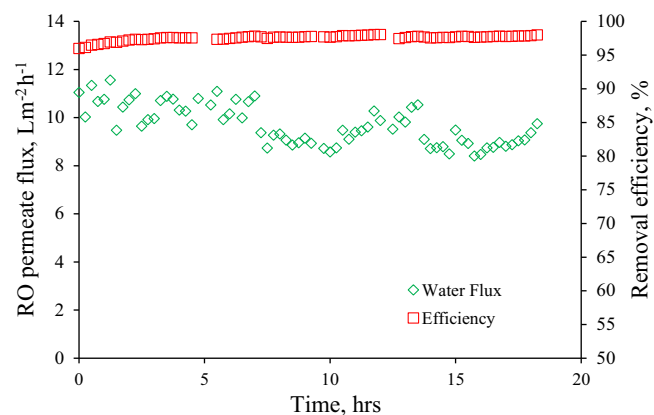
Fig. 6. RO efficiency and water flux for the integrated FO–RO system (operating pressure 30 bar).

In the next step of the extended operation testing, the integrated bench scale FO–RO unit was put through a rigorous performance evaluation by operating over an eight day period to observe the stability of the FO and RO flux and permeate production. Mine water MW2 was used against a draw solution of 0.25 M SHMP in PRO mode. SHMP was selected as draw solution even though it has a slightly lower FO flux than DHSP, as it has a higher rejection rate when used in the RO system.

The integrated system was operated by recirculating a fraction of the RO reject stream to the draw solution and bypassing a portion of diluted draw solution from the FO unit to the RO feed. The amount of diluted FO draw bypass to the RO feed was set to match the FO permeate flux and the reject return to the FO draw, thereby keeping the volume of FO draw solution constant. This mode of operation was adopted in this study so that this method can be applied for operation under field conditions in the future. No chemical cleaning was adopted with the only mode of cleaning adopted being circulating clean water once at the end of each day of operation (as identified in the previous experiment). The average FO feed flux, final feed conductivity and the average RO permeate quality for each day are presented in Table 7.

Under the study conditions adopted, the experimental results showed that over the course of eight days, raw mine water was concentrated at a steady rate and a stable flow of reusable quality clean water was obtained as RO permeate. The experiment was continuously run until the feed water (raw mine impacted water), was successfully concentrated to 20% of the starting volume. As shown in Table 7, during the integrated FO–RO operation, the FO flux rate did decline gradually over the course of the experiment (from 4.8 to 2.08 $Lm^{-2} h^{-1}$), due to the reduction in the osmotic gradient. The overall salt removal efficiency was over 97%, delivering a final treated water with an average permeate conductivity of 371 $\mu S\ cm^{-1}$ with a SHMP draw solution of 0.25 M concentration (draw solution conductivity of 40.1 $mS\ cm^{-1}$). To investigate further on the FO flux decline, a fresh FO membrane was tested with feed and draw solutions of the same concentration as those on day 8 and the flux was found to be 2.2 $Lm^{-2} h^{-1}$. This indicates that the decline in FO flux was largely due to the reduction in the osmotic gradient over the course of the long term experiment.

The concentration of the feed solution to 20% of the starting volume with no appreciable loss in RO permeate flow rate has demonstrated that this FO–RO integrated process has a potential to treat wide range of feed water concentrations. Furthermore, the draw solution successfully concentrated the feed water even though the membrane was exposed to raw mine wastewater for several days without needing chemical cleaning to the membrane. The FO membrane sample was also examined through SEM image after eight days of testing (Fig. 7).

Investigation of the SEM images of the FO membrane surface (Fig. 7) after the study duration showed no apparent strongly adhered deposit layer on the surface. As the mine water was not forced through the membrane, material deposit on the membrane was minimised. This is also one of the advantages in adopting FO as a method of pre-treatment.
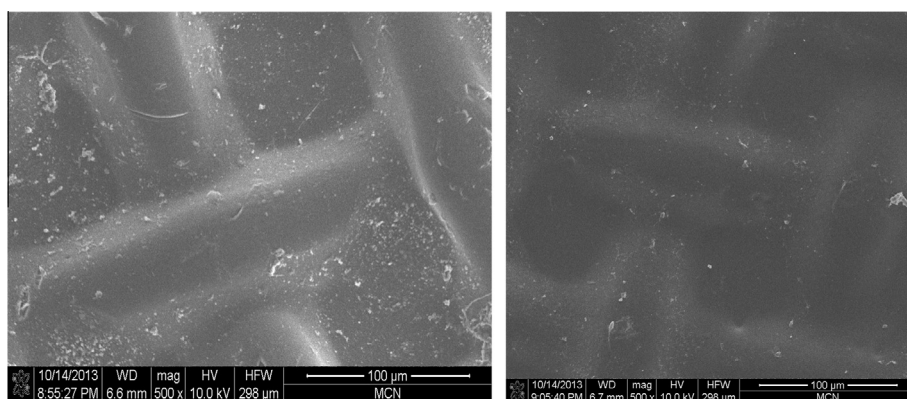
3.3. Effect of temperature on FO/RO system

Although the temperatures of the FO and RO units were maintained at 25 °C during the course of this study, the influence increased temperature on the performance of the system was also examined. Firstly testing with each unit individually and then with the combined FO–RO system to determine the absolute increase in permeate rate when combining the system. This increase should be twofold, not only the increase due to temperature from each individual unit but also the increase in permeate through the FO membrane should dilute the draw solution/RO feed further which will lead to a further increase in the production of RO permeate, above the increase caused by temperature alone, as lower concentration solutions at the same hydraulic pressure produce more permeate. The draw solution chosen for the temperature work was SHMP (0.25 M) as this was the draw solution chosen for the long term experiments. The FO feed solution chosen for these experiments was MW2.

The temperature variation did show an increase in permeate rates as expected. For the RO unit this is understood to occur due to a decrease in the viscosity leading this pressure driven process to force more water through the membrane (with the decrease in resistance). The experiments showed that while the increase due to temperature alone is 1–2% per °C, the increase due to pressure is on the order of 10% per bar, demonstrating that it is a pressure driven process. FO, which showed an increase of 2–3% per °C, on the other hand is not a pressure driven process and in this instance

Table 7
Performance of the FO–RO integrated system over eight days of operation.

Day	Average FO flux, $Lm^{-2} h^{-1}$	Final feed conductivity, $mS\ cm^{-1}$	Average RO permeate quality, $\mu S\ cm^{-1}$
1	4.8	11.45	324
2	4.4	12.59	295
3	4.12	13.95	270
4	3.64	15.47	381
5	3.2	16.81	349
6	2.8	18.69	443
7	2.36	21.75	452
8	2.08	23.61	455

Fig. 7. SEM image of the support and rejection layer of the FO membrane after extended operation.

Table 8
The effect of temperature on the integrated FO–RO system (feed MW2, draw SHMP 0.25 M, RO 20 bar).

Temperature profile (FO feed-FO draw-RO feed), °C	FO flux, $Lm^{-2}h^{-1}$	RO permeate flux, $Lm^{-2}h^{-1}$
25–25–25	3.2	3.81
25–35–25	4.0	4.11
25–35–35	4.0	4.45

the most likely cause for the increase in permeate rate is actually an increase in the osmotic pressure (as FO is an osmotically driven process). The Morse equation [59–61], used to calculate osmotic pressure, has a temperature component which is directly proportional to the osmotic pressure. As a result, when the temperature goes up, the osmotic pressure goes up, which would draw more permeate across the membrane. Similar increases in FO and RO performance with the increase in temperature have also been reported earlier [66–68]. The increase in RO permeate flow with pressure, between 20 and 30 bar, was found to be 10–15% per bar.

The energy use of both the feed and draw FO pumps and the high pressure RO variable speed pump was also monitored during the course of this study. It was found that through this preliminary evaluation the FO process utilised about 17% of the overall energy use of the RO process. However, it is to be noted that the lab scale system uses low performance pumps and there are no energy recovery systems in place.

The effect of temperature on the combined system was then evaluated. In these experiments, the RO system was kept at a constant hydraulic pressure (20 bar) and the RO feed and FO draw temperatures were varied as shown in Table 8. The system was operated in constant volume mode with a slightly higher RO pressure. This method of integration was chosen so that the FO and RO flux rates would be of similar magnitude which would allow any increases in the RO flux caused by the increase in FO flux to be clearly seen.

When the units were integrated it showed that an increase in the FO draw temperature alone would lead to an increase in the RO permeate rate without the need of heating the RO feed. The best configuration was when the RO feed and FO draw were heated. These results demonstrate that heating the FO draw solution leads to a double flow on effect, firstly due to the increased FO permeate rate increasing the rate at which the RO feed is diluted and secondly the increase in permeate that is seen for RO when the feed is heated. The best configuration to get the most of the combined effect would just be to heat the FO draw solution/RO feed solution. This would maximise the osmotic gradient between the FO feed and draw, yielding maximum dilution of the RO feed solution which coupled with the reduction in viscosity would lead to the maximum RO permeate.

4. Conclusions

An integrated forward and reverse osmosis process was applied to treat three different types of actual coal mine impacted waters. Two methods of integration, namely the constant volume and constant concentration modes were identified in this study and each was found to have its own advantages. The combination of FO with RO provided a better performance than FO-only or RO-only systems. Mine water was treated with the integrated system over an extended duration and the feed was concentrated to 20% of its starting volume. During the course of these studies, an alternative method for the determination of osmotic pressure for a given solution was developed. The effect of temperature on the efficiency of the integrated process was also determined and the optimal temperature configuration was found to be achieved by elevating the draw solution temperature. This technology offers mine sites a readily controllable onsite water treatment method that can be tailored to each site's water management requirements.

References

[1] P. Cashin, K. Mohaddes, M. Raissi, Fair weather or foul? The macroeconomics effect of El Nino., Cambridge working papers in economics, University of Cambridge, 2014.
[2] S. Vink, S. Robbins, Mine water management in variable climate regimes, in: C. D. McCullough, M.A. Lund, L. Wyse (Eds.), International Mine Water Association Symposium. Annual Conference 2012, International Mine Water Association, Bunbury, Australia, 2012. 20A-20I.
[3] R. Thiruvenkatachari, M. Younes, S. Su, Coal mine site investigation of wastewater quality in Australia, Desalination Water Treatment 32 (2011) 357–364.
[4] M. Hoang, B. Bolto, C. Haskard, O. Barron, S. Gray, G. Leslie, Desalination in Australia, 2009, pp. 26.
[5] L.F. Greenlee, D.F. Lawler, B.D. Freeman, B. Marrot, P. Moulin, Reverse osmosis desalination: water sources, technology, and today's challenges, Water Res. 43 (2009) 2317–2348.
[6] S. Burn, M. Hoang, D. Zarzo, F. Olewniak, E. Campos, B. Bolto, O. Barron, Desalination techniques — a review of the opportunities for desalination in agriculture, Desalination 364 (2015) 2–16.
[7] INAP, Treatment of sulphate in mine effluents, 2003.
[8] U. EPA, Reference guide to treatment technologies for mining-influenced waters, USA, 2014.
[9] G.M. Mustafa, The study of pretreatment options for composite fouling of reverse osmosis membranes used in water treatment and production, Chemical Sciences & Engineering, Faculty of Engineering, University of New South Wales, Australia, 2007.
[10] S. Muraleedaaran, X. Li, L. Li, R. Lee, Is reverse osmosis effective for produced water purification? Viability and economic analysis., 2009 SPE Western Regional Meeting, Society of Petroleum Engineers, San Jose, California, USA, 2009.
[11] E.-S. Kim, Y. Liu, M. Gamal El-Din, The effects of pretreatment on nanofiltration and reverse osmosis membrane filtration for desalination of oil sands process-affected water, Sep. Purif. Technol. 81 (2011) 418–428.
[12] V. Bonnélye, L. Guey, J. Del Castillo, UF/MF as RO pre-treatment: the real benefit, Desalination 222 (2008) 59–65.
[13] T.Y. Cath, A.E. Childress, M. Elimelech, Forward osmosis: Principles, applications, and recent developments, J. Membr. Sci. 281 (2006) 70–87.
[14] M. Qasim, N.A. Darwish, S. Sarp, N. Hilal, Water desalination by forward (direct) osmosis phenomenon: a comprehensive review, Desalination 374 (2015) 47–69.
[15] S. Zhao, L. Zou, C.Y. Tang, D. Mulcahy, Recent developments in forward osmosis: opportunities and challenges, J. Membr. Sci. 396 (2012) 1–21.
[16] H. Luo, Q. Wang, T.C. Zhang, T. Tao, A. Zhou, L. Chen, X. Bie, A review on the recovery methods of draw solutes in forward osmosis, J. Water Process Eng. 4 (2014) 212–223.
[17] S. Phuntsho, S. Hong, M. Elimelech, H.K. Shon, Forward osmosis desalination of brackish groundwater: meeting water quality requirements for fertigation by integrating nanofiltration, J. Membr. Sci. 436 (2013) 1–15.
[18] S. Phuntsho, H.K. Shon, S. Hong, S. Lee, S. Vigneswaran, A novel low energy fertilizer driven forward osmosis desalination for direct fertigation: evaluating the performance of fertilizer draw solutions, J. Membr. Sci. 375 (2011) 172–181.
[19] K.Y. Wang, Q. Yang, T.S. Chung, R. Rajagopalan, Enhanced forward osmosis from chemically modified polybenzimidazole (PBI) nanofiltration hollow fiber membranes with a thin wall, Chem. Eng. Sci. 64 (2009) 1577–1584.
[20] A. Soroush, W. Ma, Y. Silvino, M.S. Rahaman, Surface modification of thin film composite forward osmosis membrane by silver-decorated graphene-oxide nanosheets, Environ. Sci.: Nano 2 (2015) 395–405.
[21] C. Qiu, S. Qi, C.Y. Tang, Synthesis of high flux forward osmosis membranes by chemically crosslinked layer-by-layer polyelectrolytes, J. Membr. Sci. 381 (2011) 74–80.
[22] L. Setiawan, R. Wang, K. Li, A.G. Fane, Fabrication of novel poly(amide-imide) forward osmosis hollow fiber membranes with a positively charged nanofiltration-like selective layer, J. Membr. Sci. 369 (2011) 196–205.

[23] N.N. Bui, J.R. McCutcheon, Hydrophilic nanofibers as new supports for thin film composite membranes for engineered osmosis, Environ. Sci. Technol. 47 (2013) 1761–1769.

[24] J. Li, L. Yin, G. Qiu, X. Li, Q. Liu, J. Xie, A photo-bactericidal thin film composite membrane for forward osmosis, J. Mater. Chem. A 3 (2015) 6781–6786.

[25] A. Achilli, T.Y. Cath, A.E. Childress, Selection of inorganic-based draw solutions for forward osmosis applications, J. Membr. Sci. 364 (2010) 233–241.

[26] J.R. McCutcheon, R.L. McGinnis, M. Elimelech, A novel ammonia-carbon dioxide forward (direct) osmosis desalination process, Desalination 174 (2005) 1–11.

[27] M.M. Ling, T.-S. Chung, Desalination process using super hydrophilic nanoparticles via forward osmosis integrated with ultrafiltration regeneration, Desalination 278 (2011) 194–202.

[28] H.T. Nguyen, N.C. Nguyen, S.-S. Chen, H.H. Ngo, W. Guo, C.-W. Li, A new class of draw solutions for minimizing reverse salt flux to improve forward osmosis desalination, Sci. Total Environ. 538 (2015) 129–136.

[29] K. Lutchmiah, A.R.D. Verliefde, K. Roest, L.C. Rietveld, E.R. Cornelissen, Forward osmosis for application in wastewater treatment: a review, Water Res. 58 (2014) 179–197.

[30] K.L. Hickenbottom, N.T. Hancock, N.R. Hutchings, E.W. Appleton, E.G. Beaudry, P. Xu, T.Y. Cath, Forward osmosis treatment of drilling mud and fracturing wastewater from oil and gas operations, Desalination 312 (2013) 60–66.

[31] S. Zhang, P. Wang, X. Fu, T.-S. Chung, Sustainable water recovery from oily wastewater via forward osmosis-membrane distillation (FO-MD), Water Res. 52 (2014) 112–121.

[32] R.W. Holloway, A.E. Childress, K.E. Dennett, T.Y. Cath, Forward osmosis for concentration of anaerobic digester centrate, Water Res. 41 (2007) 4005–4014.

[33] X. Zhang, Z. Ning, D.K. Wang, J.C. Diniz da Costa, Processing municipal wastewaters by forward osmosis using CTA membrane, J. Membr. Sci. 468 (2014) 269–275.

[34] R. Valladares Linares, Z. Li, M. Abu-Ghdaib, C.-H. Wei, G. Amy, J.S. Vrouwenvelder, Water harvesting from municipal wastewater via osmotic gradient: an evaluation of process performance, J. Membr. Sci. 447 (2013) 50–56.

[35] Oasys applies FO to treat wastewater from China's growing power market, Membrane Technology 2014 (2014), pp. 2–3.

[36] R. Kumar, P. Pal, A novel forward osmosis-nano filtration integrated system for coke-oven wastewater reclamation, Chem. Eng. Res. Des. 100 (2015) 542–553.

[37] P. Zhao, B. Gao, S. Xu, J. Kong, D. Ma, H.K. Shon, Q. Yue, P. Liu, Polyelectrolyte-promoted forward osmosis process for dye wastewater treatment – Exploring the feasibility of using polyacrylamide as draw solute, Chem. Eng. J. 264 (2015) 32–38.

[38] S. Adham, J. Oppenheimer, L. Liu, M. Kumar, Dewatering Reverse Osmosis Concentrate from Water Reuse Applications Using Forward Osmosis, 2007.

[39] H.H. Salih, L. Wang, V. Patel, V. Namboodiri, K. Rajagopalan, The utilization of forward osmosis for coal tailings dewatering, Miner. Eng. 81 (2015) 142–148.

[40] H. Kyllonen, E. Jarvela, A. Gronroos, M. Arnold, Forward osmosis as a part of mining water concepts, Membrane Conference and Exposition Las Vegas, USA, 2014.

[41] A. Altaee, A. Mabrouk, K. Bourouni, P. Palenzuela, Forward osmosis pretreatment of seawater to thermal desalination: high temperature FO-MSF/MED hybrid system, Desalination 339 (2014) 18–25.

[42] K.Y. Wang, M.M. Teoh, A. Nugroho, T.-S. Chung, Integrated forward osmosis–membrane distillation (FO–MD) hybrid system for the concentration of protein solutions, Chem. Eng. Sci. 66 (2011) 2421–2430.

[43] O.A. Bamaga, A. Yokochi, B. Zabara, A.S. Babaqi, Hybrid FO/RO desalination system: preliminary assessment of osmotic energy recovery and designs of new FO membrane module configurations, Desalination 268 (2011) 163–169.

[44] T.Y. Cath, J.E. Drewes, C.D. Lundin, N.T. Hancock, Forward osmosis—reverse osmosis process offers a novel hybrid solution for water purification and reuse, IDA J. Desalination Water Reuse 2 (2010) 16–20.

[45] S. Zhao, L. Zou, D. Mulcahy, Brackish water desalination by a hybrid forward osmosis–nanofiltration system using divalent draw solute, Desalination 284 (2012) 175–181.

[46] T.Y. Cath, J.E. Drewes, C. Lundin, A novel hybrid forward osmosis – reverse osmosis process for water purification and reuse, using impaired water and saline water, 2009 AWWA Membrane Technology Conference and Exposition, 2009.

[47] D.L. Shaffer, N.Y. Yip, J. Gilron, M. Elimelech, Seawater desalination for agriculture by integrated forward and reverse osmosis: improved product water quality for potentially less energy, J. Membr. Sci. 415–416 (2012) 1–8.

[48] Y.-J. Choi, J.-S. Choi, H.-J. Oh, S. Lee, D.R. Yang, J.H. Kim, Toward a combined system of forward osmosis and reverse osmosis for seawater desalination, Desalination 247 (2009) 239–246.

[49] A. Altaee, G. Zaragoza, H.R. van Tonningen, Comparison between forward osmosis-reverse osmosis and reverse osmosis processes for seawater desalination, Desalination 336 (2014) 50–57.

[50] S. Jamil, P. Loganathan, C. Kazner, S. Vigneswaran, Forward osmosis treatment for volume minimisation of reverse osmosis concentrate from a water reclamation plant and removal of organic micropollutants, Desalination 372 (2015) 32–38.

[51] N.T. Hancock, T.Y. Cath, Solute coupled diffusion in osmotically driven membrane processes, Environ. Sci. Technol. 43 (2009) 6769–6775.

[52] W.A. Phillip, J.S. Yong, M. Elimelech, Reverse draw solute permeation in forward osmosis: modeling and experiments, Environ. Sci. Technol. 44 (2010) 5170–5176.

[53] N. Cini, V. Ball, Polyphosphates as inorganic polyelectrolytes interacting with oppositely charged ions, polymers and deposited on surfaces: fundamentals and applications, Adv. Colloid Interface Sci. 209 (2014) 84–97.

[54] D.E. Abd-El-Khalek, B.A. Abd-El-Nabey, Evaluation of sodium hexametaphosphate as scale and corrosion inhibitor in cooling water using electrochemical techniques, Desalination 311 (2013) 227–233.

[55] J. Duan, E. Litwiller, S.-H. Choi, I. Pinnau, Evaluation of sodium lignin sulfonate as draw solute in forward osmosis for desert restoration, J. Membr. Sci. 453 (2014) 463–470.

[56] D. Yang, H. Li, Y. Qin, R. Zhong, M. Bai, X. Qiu, Structure and properties of sodium lignosulfonate with different molecular weight used as dye dispersant, J. Dispersion Sci. Technol. 36 (2015) 532–539.

[57] O.S. Inc., StreamAnalyzer 2.0 & Electrolyte Package, Morris Plains, NJ, USA.

[58] J.R. McCutcheon, M. Elimelech, Influence of concentrative and dilutive internal concentration polarization on flux behavior in forward osmosis, J. Membr. Sci. 284 (2006) 237–247.

[59] A.D. Wilson, F.F. Stewart, Deriving osmotic pressures of draw solutes used in osmotically driven membrane processes, J. Membr. Sci. 431 (2013) 205–211.

[60] H.N. Morse, The Osmotic Pressure of Aqueous Solutions: Report on Investigations Made in the Chemical Laboratory of the Johns Hopkins University during the years 1899–1913, Carnegie Institution of Washington, USA, 1914.

[61] A. Findley, Osmotic Pressure, Longmans, Green and Co, 1919.

[62] J.R. McCutcheon, M. Elimelech, Modeling water flux in forward osmosis: implications for improved membrane design, AIChE J. 53 (2007) 1736–1744.

[63] Y. Xu, X. Peng, C.Y. Tang, Q.S. Fu, S. Nie, Effect of draw solution concentration and operating conditions on forward osmosis and pressure retarded osmosis performance in a spiral wound module, J. Membr. Sci. 348 (2010) 298–309.

[64] G.T. Gray, J.R. McCutcheon, M. Elimelech, Internal concentration polarization in forward osmosis: role of membrane orientation, Desalination 197 (2006) 1–8.

[65] S. Lee, C. Boo, M. Elimelech, S. Hong, Comparison of fouling behavior in forward osmosis (FO) and reverse osmosis (RO), J. Membr. Sci. 365 (2010) 34–39.

[66] M.F.A. Goosen, S.S. Sablani, S.S. Al-Maskari, R.H. Al-Belushi, M. Wilf, Effect of feed temperature on permeate flux and mass transfer coefficient in spiral-wound reverse osmosis systems, Desalination 144 (2002) 367–372.

[67] S. Zhao, L. Zou, Effects of working temperature on separation performance, membrane scaling and cleaning in forward osmosis desalination, Desalination 278 (2011) 157–164.

[68] S. Phuntsho, S. Vigneswaran, J. Kandasamy, S. Hong, S. Lee, H.K. Shon, Influence of temperature and temperature difference in the performance of forward osmosis desalination process, J. Membr. Sci. 415–416 (2012) 734–744.